catalysts

MDPI

Article

Catalytic Conversion of Glycerol to Methyl Lactate over Au-CuO/Sn-Beta: The Roles of Sn-Beta

Ying Duan [1], Qianqian Luo [2], Renfeng Nie [2], Jianshe Wang [2], Yongsheng Zhang [2], Tianliang Lu [2,*] and Chunbao Xu [3,*]

[1] College of Food and Drug, Luoyang Normal University, Luoyang 471934, China; duanying@mail.ustc.edu.cn
[2] School of Chemical Engineering, Zhengzhou University, Zhengzhou 450001, China; luoqianqian2022@163.com (Q.L.); refinenie@163.com (R.N.); jianshewang@zzu.edu.cn (J.W.); yongshengzhang001@163.com (Y.Z.)
[3] Department of Chemical and Biochemical Engineering, Western University, 1151 Richmond St., London, ON N6A 3K7, Canada
* Correspondence: lutianliang@zzu.edu.cn (T.L.); cxu6@uwo.ca (C.X.)

Abstract: The production of methyl lactate as a degradable polymer monomer from biomass was an important topic for a sustainable society. In this manuscript, glycerol was oxidated to methyl lactate catalyzed by the combination of Au-CuO and Sn-Beta. The influence of Sn content, Sn source, and the preparation conditions for Sn-β was studied. The Au content in Au/CuO was also investigated by varying the Au content in Au/CuO. The catalysts were characterized by XRD, FTIR spectroscopy of pyridine adsorption, and TEM to study the role of Sn and the influence of different parameters for catalyst preparation. After the optimization of reaction parameters, the yield of methyl lactate from glycerol reached 59% at 363 K after reacting in 1.6 MPa of O_2 for 6 h.

Keywords: glycerol; oxidation; methyl lactate; Sn-Beta; Au/CuO

check for updates

Citation: Duan, Y.; Luo, Q.; Nie, R.; Wang, J.; Zhang, Y.; Lu, T.; Xu, C. Catalytic Conversion of Glycerol to Methyl Lactate over Au-CuO/Sn-Beta: The Roles of Sn-Beta. *Catalysts* **2022**, *12*, 104. https://doi.org/10.3390/catal12010104

Academic Editor: Gloria Fernandez-Lorente

Received: 30 November 2021
Accepted: 12 January 2022
Published: 17 January 2022

Publisher's Note: MDPI stays neutral with regard to jurisdictional claims in published maps and institutional affiliations.

Copyright: © 2022 by the authors. Licensee MDPI, Basel, Switzerland. This article is an open access article distributed under the terms and conditions of the Creative Commons Attribution (CC BY) license (https://creativecommons.org/licenses/by/4.0/).

1. Introduction

The demand for energy and materials is increasing with the rapid development of society. While promoting the development of humans, the utilization of fossil fuels has resulted in a series of problems, such as environmental, carbon emission, non-biodegradable polymers, and so on. In this regard, the utilization of renewable biomass resources for environmentally friendly products is attracting more and more attention [1–4]. For example, Diol [5–8], dibasic acid [9–12] and diamine [13–15] as polymer monomer and cyclopentanone derivatives [16–20] as high value-added fine chemicals could be obtained from biomass; 2,5-dimethylfuran [21–23], which originated from carbohydrates, was a promising fuel candidate. Millions of tons of biodiesel were produced from the transesterification of fatty acids with methanol every year [24,25]. The sustainable and environmental-friendly characters made biodiesel a promising alternative to fossil-based diesel.

Abundant glycerol (GLY) was produced as by-products during the production of biodiesel. The utilization of GLY was an interesting topic of scientific and economic significance. A lot of research had focused on the topic and propanediol [26–28], lactic acid [29–44], 1,3-dihydroxyacetone (DHA) [45–54], and glycerol acid [55] were the typical products obtained from GLY. Lactic acid and its ester were considered as one of the main building blocks as lactic acid (ester) could be converted to various valuable chemicals. Polylactic acid is a biodegradable polymer with good mechanical properties and chemical and thermal stability. What is more, considering the whole cycle, no additional carbon was discharged when polylactic acid was used. So, the conversion of GLY to lactic acid was of great significance for both the utilization of biodiesel by-products and the production of biodegradable polymers. There were a number of examples for the transformation of GLY to lactic acid. For example, Sharninghausen et al. reported a family of iridium complexes

as homogeneous catalysts for the conversion of glycerol to lactic acid without solvent [43]. Recently, we found that glycerol could be converted to methyl lactate (MLA) with the multifunctional Au/Sn-USY catalyst [44].

Based on the literature and our study, two functions were needed for the catalyst to transform GLY into lactic acid. One is the oxidation function that could oxidate the glycerol to DHA while the other is the acid site that could convert the DHA to lactic acid. The noble metal catalyst, as well as non-noble metal catalyst, had been proven to be effective for the oxidation of GLY to DHA [45–54]. Typically, the Au, Pt, Pd and Cu were well used for this transformation. Dong et al. explored the support effect for supported Au catalysts in the oxidation of GLY to DHA; a 73.5% yield of DHA was obtained on Au/CuO catalysts [56]. The isomerization of DHA to lactic acid was usually catalyzed by Lewis acid. Though the homogeneous Lewis acid showed good activity and selectivity to lactic acid, the solid acid was preferred due to its separability and reusability [57–60]. The Sn containing molecular sieve usually showed a good effect for the isomerization of DHA to lactic acid [61,62]. Feliczak-Guzik et al. reported that a high yield of alkyl lactates and lactic acid could be achieved by using Sn containing hierarchical zeolites [62].

As the methanol was usually in excess for the production of biodiesel, the by-product GLY was always in coexistence with methanol after the production of biodiesel. It is more meaningful to prepare MLA by the reaction of methanol and GLY. In this manuscript, GLY was directly converted to MLA by the combination of Au-CuO and Sn-Beta. The Au-CuO and Sn-Beta showed a good synergistic effect and could realize the reaction without the addition of a base. The effect of catalyst properties on the reaction was studied and discussed with the aid of catalyst characterization. Under the optimal conditions, a 59% yield of MLA was achieved.

2. Results and Discussion

2.1. Characterization

2.1.1. XRD Patterns

The XRD patterns of Sn-β prepared by different Sn sources were shown in Figure 1. All the samples showed the typical BEA structure for β zeolite. The introduction of Sn did not have much influence on the structure of β zeolite. However, the crystallinity was affected by the Sn content as well as the Sn source. As the Sn content increased, the crystallinity of Sn-β decreased for Sn-β-Cl, Sn-β-OXS, and Sn-β-DBTM revealed by the decrease in the characteristic diffraction peaks. It was reported that the increase in the content of Sn in the gel would slow down the crystallization rate of zeolite. This should be the reason for the decrease in crystallinity. This decreased trend had been strengthened when more water was given in the gel (H_2O/SiO_2 = 7.5, Figure S2). There had a sharp decrease when the Sn content was over 1% for Sn-β prepared using more water (H_2O/SiO_2 = 7.5, Figure S2) compared to the Sn-β prepared using less water (H_2O/SiO_2 = 5, Figure 1a). Compared to Sn-β-Cl and Sn-β-OXS, the Sn-β-DBTM had lower characteristic diffraction peaks, especially at high Sn content. This could be caused by the insolubilization of $C_{12}H_{20}O_4Sn$ in water.

The XRD patterns of Au/CuO-Sn-β with different Au contents were shown in Figure 2. The characteristic diffraction peaks for β zeolite were maintained after the combination of Au/CuO and Sn-β. The preparation process did not damage the structure of Sn-β zeolite. The characteristic diffraction peaks of Au and CuO could be observed by partially enlarging the XRD patterns. The characteristic diffraction peaks located at 2θ = 35.5°, 38.7° and 48.1° was ascribed to the diffraction peaks of CuO (11–1), (11–1) and (20–2) crystal planes. The characteristic diffraction peak located at 2θ = 44.4° belonged to the diffraction peak of the Au (200) crystal plane. The Au and CuO were just not affected by the preparation process.

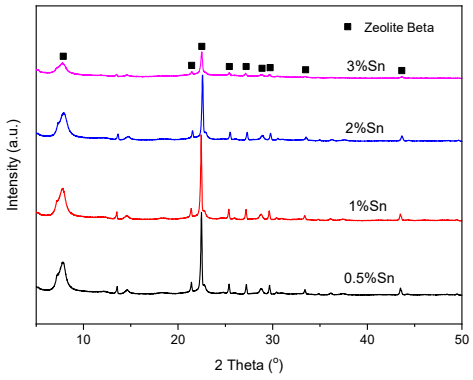

(**a**)

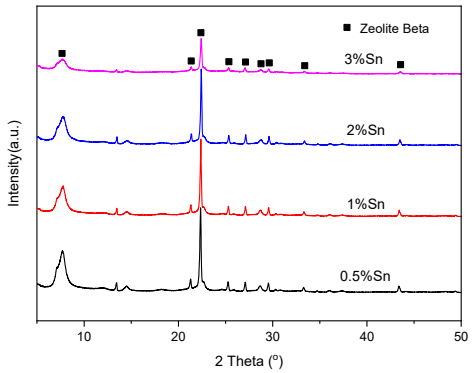

(**b**)

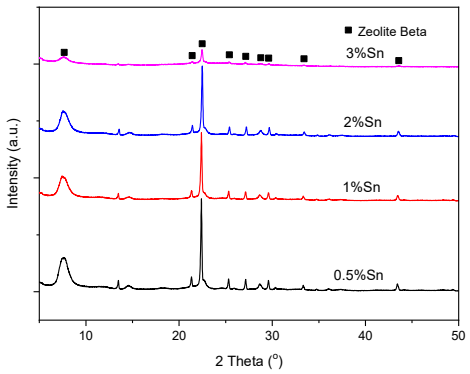

(**c**)

Figure 1. The XRD patterns of Sn-β-Cl (**a**), Sn-β-OXS (**b**), and Sn-β-DBTM (**c**).

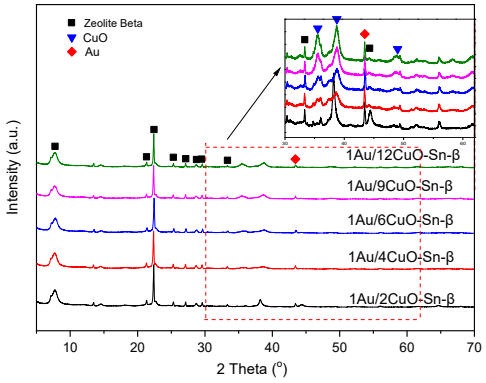

Figure 2. The XRD patterns of Au/CuO-Sn-β with different Au contents.

2.1.2. FTIR Spectroscopy of Pyridine Adsorption

FTIR spectroscopy of pyridine adsorption was used to study the acidity of the Sn-Beta (Figure 3). For all the samples, the absence of the band at 1545 cm^{-1} indicated that no Brønsted acid sites formed in these synthesized Sn-Beta. The bands at 1452 and 1490 cm^{-1} were attributed to the pyridine bound with the Lewis acid sites. Moreover, the band at 1445 cm^{-1} can be ascribed to the physical adsorption of pyridine. Considering the disruption of the band at 1445 cm^{-1}, the changing trend of the band at 1490 cm^{-1} is more convenient than that at 1452 cm^{-1} for determining the formation of L acid sites in this work. It could be seen that the intensity of the band at 1490 cm^{-1} increased while the selectivity to MLA decreased followed the order of Sn-β-Cl, Sn-β-OXS, and Sn-β-DBTM prepared from different sources of Sn (Figure 3a). As for Sn-β-Cl, when the Sn content is 0.5%, the band at 1490 cm^{-1} is very weak indicating the small amount of L acid sites. With the increase of Sn content from 0.5% to 3%, the increase of band intensity at 1490 cm^{-1} implies the increase of L acid sites amount. The introduction of Sn in Sn-β leads to the increase of L acid sites.

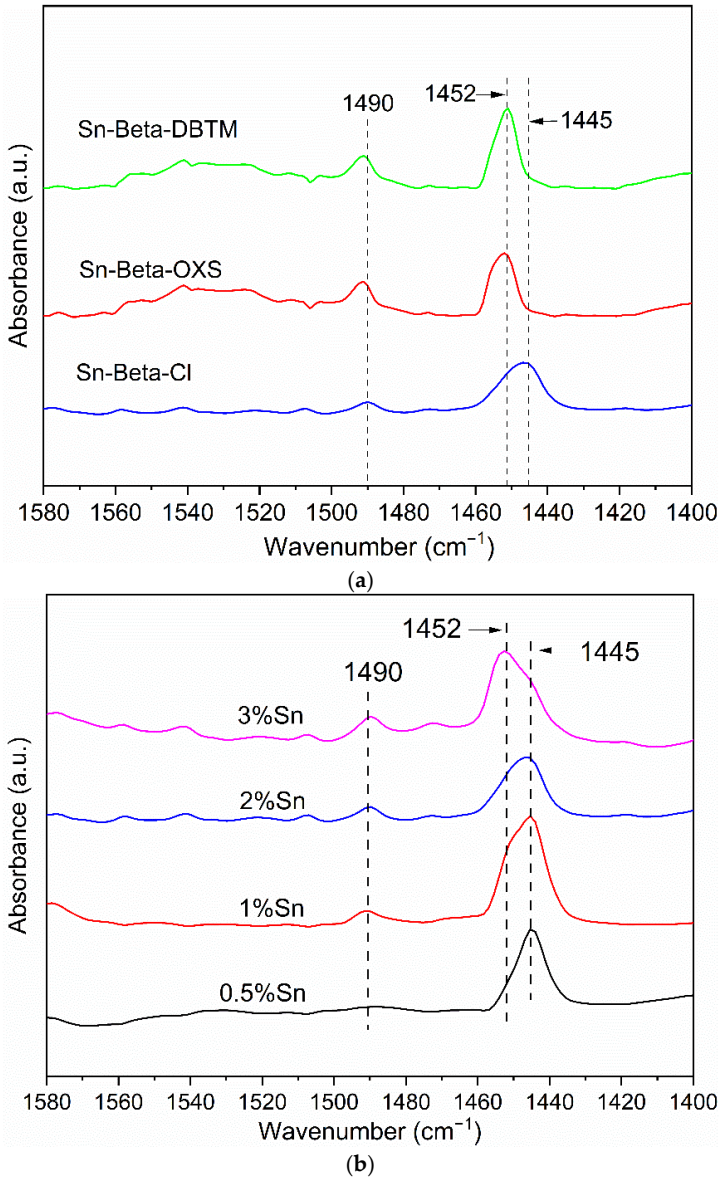

Figure 3. The FTIR spectroscopy of pyridine adsorption of Sn-β prepared from different Sn sources (**a**) and Sn-β-Cl with different Sn content (**b**).

2.1.3. TEM Images

To study the reason for the difference in activity for different Au content, the TEM images were taken for Au/CuO with different CuO contents in Au/CuO. The TEM images, as well as the particle size distribution, were exhibited in Figure 4. The particle size of Au nanoparticles was large and unevenly distributed, and the average particle size was 10.85 nm for 1Au/2CuO. When the content of Au decreased, the average particle size of Au nanoparticles was 5.45 nm. The particle size of Au nanoparticles was obviously smaller and the distribution was more uniform compared to 1Au/2CuO. The particle size of Au nanoparticles continued to decrease with the decrease in Au content. It was clear that the lower the Au content, the smaller the particle size of Au and the more uniform the distribution of Au nanoparticles.

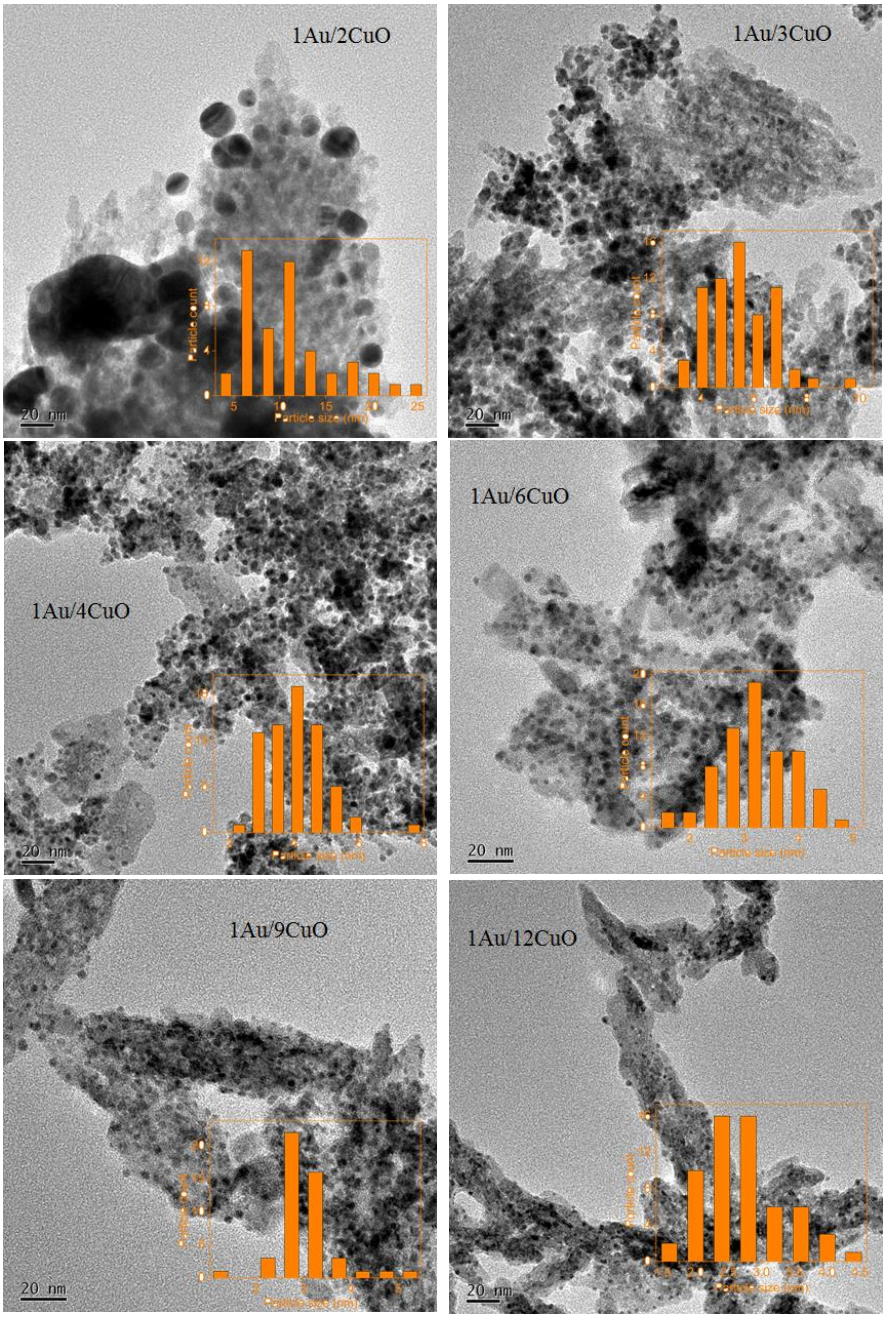

Figure 4. TEM images of Au/CuO with different CuO contents in Au/CuO.

2.2. Effect of Sn-β on the Glycerol Oxidation

2.2.1. Sn Source and Sn Content

We first studied the effect of Sn-β by simple mixing of Au/CuO and Sn-β. The effect of the Sn was studied by using different Sn sources with various Sn content. The products distribution was shown in Tables S1–S3. As the over-oxidation products, methyl glycerate (GLR) and methyl pyruvate (MP) were the by-products. When Al-β without Sn was used accompanied with Au/CuO, 97% of GLY was converted after reacting for 4 h at 363 K (Figure 5). This showed that Au/CuO was of high activity for the oxidation of GLY. However, only 3% selectivity to MLA was obtained after the reaction (Figure 5 and Table S1, Entries 1). The combination of Au/CuO and Al-β was not effective for obtaining MLA from GLY. When Sn was added to the β molecular sieve, the conversion of GLY was maintained at around 95%. This illustrated that the addition of Sn did not influence the activity of Au/CuO. However, the selectivity to MLA was enhanced a lot compared to the Al-β without Sn. When 0.5% of Sn was added, the selectivity to MLA increased to 38% on Sn-β-Cl which was prepared using $SnCl_4$ as the Sn source (Figure 5). As the content of Sn increased from 0.5% to 2.0% in Sn-β-Cl, the selectivity to MLA increased from 38% to 60%. When the content of Sn continued to increase to 3.0%, the selectivity to MLA decreased a little to 44%. It was clear that appropriate Sn content was a necessity for high selectivity to MLA. With the increase of Sn content from 0.5% to 3%, the increase of band intensity at 1490 cm^{-1} implies the increase of L acid site amount revealed by the results of FTIR spectroscopy of pyridine adsorption (Figure 3). The L acid sites were the active center for isomerization of DHA to MLA. The excess L acid center might promote the side reaction thus was not conducive to high selectivity to MLA. This was also proved by preparing the Sn-β with different Sn sources. Both Sn-β-OXS and Sn-β-DBTM had higher L acid amounts than Sn-β-Cl (Figure 3a); however, they had lower selectivity to MLA (Figure 5). We further studied the conversion of GLY to MLA using Sn-β with different Sn sources. It could be seen in Figure 5 that the conversion of GLY was maintained when the Sn-β was prepared using different Sn sources. However, when SnC_2O_4 and $C_{12}H_{20}O_4Sn$ were selected as the Sn sources to prepare Sn-β-OXS and Sn-β-DBTM, the selectivity to MLA had similar trends as Sn-β which was prepared using $SnCl_4$ as Sn source. When the Sn content was lower than 2.0%, the selectivity to MLA increased with the increase of Sn content. Then the selectivity to MLA decreased when the content of Sn continued to increase to 3.0%. However, the Sn source did have an influence on the selectivity to MLA. When $C_{12}H_{20}O_4Sn$ was used, the selectivity to MLA was lower at various Sn contents compared to Sn-β-Cl and Sn-β-OXS which was prepared using $SnCl_4$ and SnC_2O_4 as an Sn source. This difference should be caused by the difference in the solubility for $SnCl_4$, SnC_2O_4 and $C_{12}H_{20}O_4Sn$. The $C_{12}H_{20}O_4Sn$ is insoluble in water which caused an uneven distribution of Sn on Sn-β-DBTM.

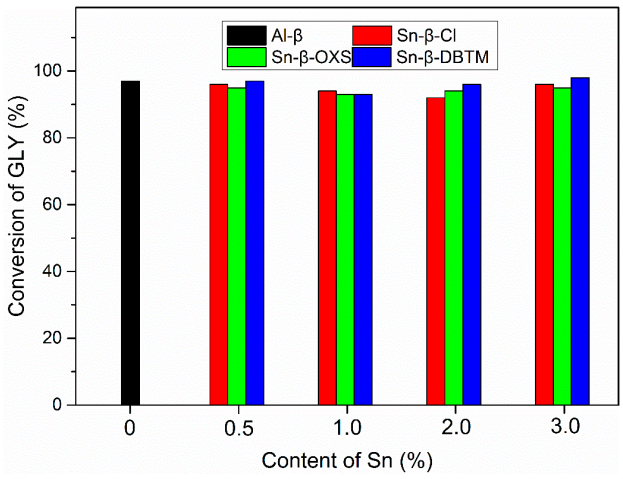

Figure 5. *Cont.*

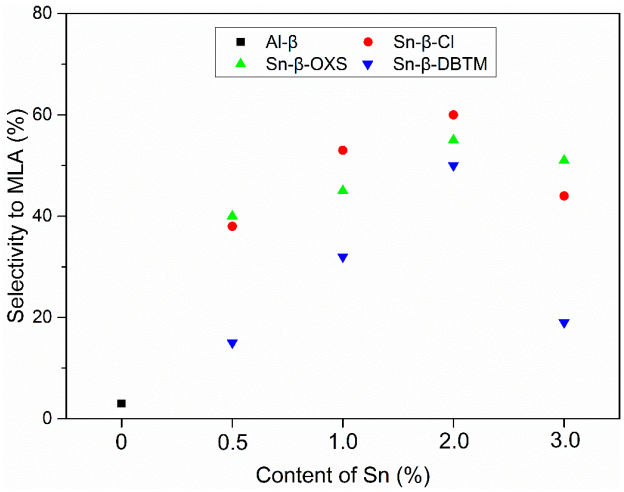

Figure 5. The effect of Sn on the GLY oxidation.

2.2.2. Preparation of Sn-β with Different Content of H_2O in the Gel

The H_2O had a great influence on the preparation of Sn-β. Herein, we adjusted the water content in the gel while the proportion of other components remained unchanged to study the influence of water. The water content in the gel was settled at H_2O/SiO_2 = 5 and 7.5. The results were shown in Figure 6. The conversion of GLY was not affected vary the Sn-β was prepared with H_2O/SiO_2 = 5 and 7.5. The Sn-β did not affect the activity of Au/CuO. Both of the prepared Sn-β with H_2O/SiO_2 = 5 and 7.5 showed high selectivity to MLA at appropriate Sn content. There was a difference in the relationship between Sn content and selectivity to MLA. The highest 60% selectivity to MLA occurred at 2% content of Sn for H_2O/SiO_2 = 5 while 63% was achieved at 1% content of Sn for H_2O/SiO_2 = 7.5. This difference should be explained by the XRD results (Figure 1a and Figure S2). The sharp decrease when the Sn content was over 1% for Sn-β prepared using more water (H_2O/SiO_2 = 7.5, Figure S2) showed that the degree of crystallization was reduced when the Sn content was over 1%. However, the decrease in the degree of crystallization for the Sn-β prepared using less water (H_2O/SiO_2 = 5, Figure 1a) occurred when the Sn content was over 2%. This decrease in the degree of crystallization led to a decrease in the selectivity to MLA. The H_2O in the gel for preparation of Sn-β had a great influence on the selectivity to MLA by affecting the degree of crystallization. The Sn-β with 1% content of Sn prepared at H_2O/SiO_2 = 7.5 was used for the subsequent study. The preparation scale of Sn-β was expanded to 50 times to study the enlargement effect. It was found that the Sn-β with enlarged scale showed a catalytic effect similar to that of the catalyst before being enlarged (Table S4).

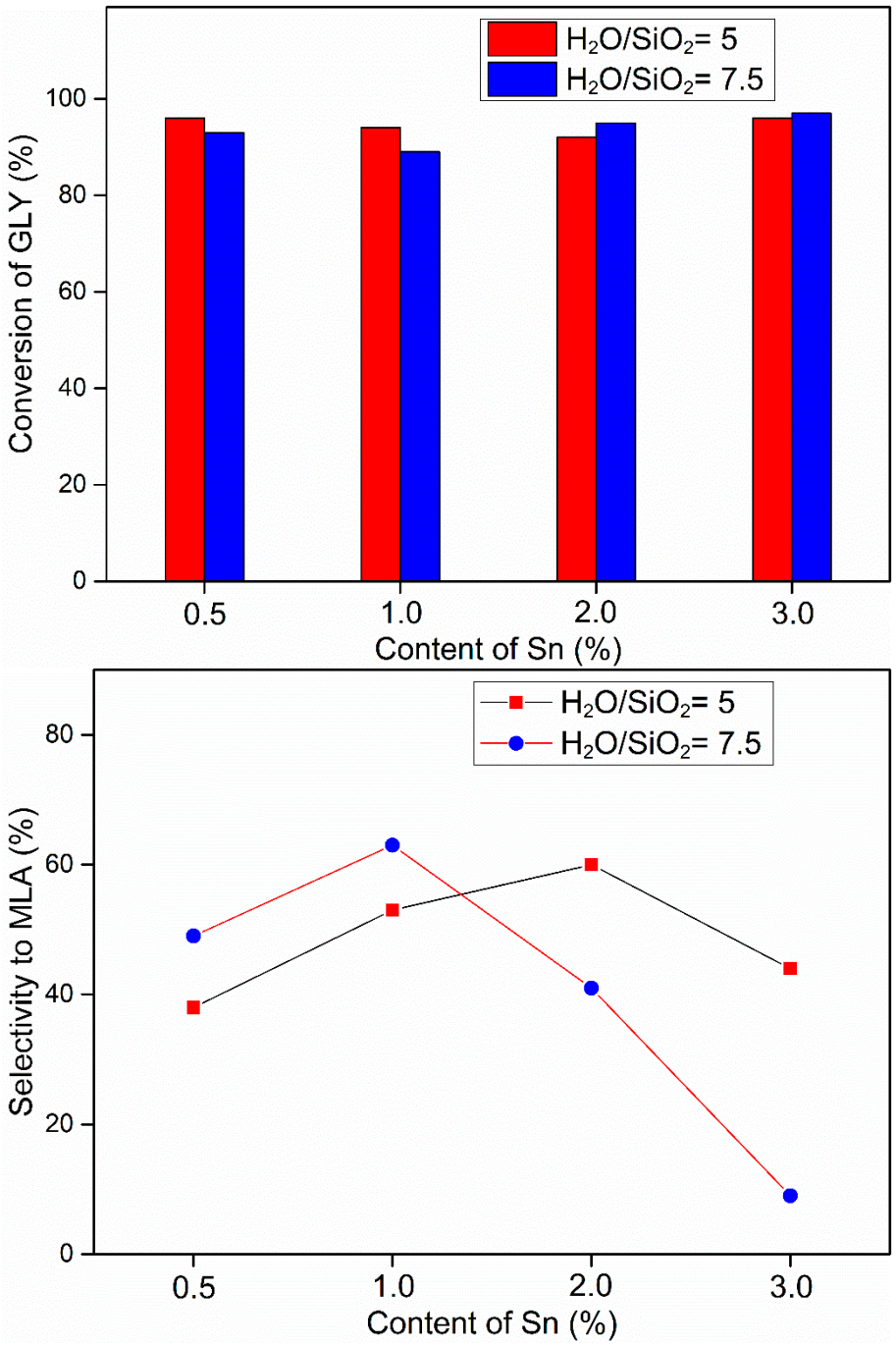

Figure 6. The GLY oxidation using Sn-β prepared with different content of H_2O.

2.3. Effect of Au/CuO on the GLY Oxidation

Au/CuO-Sn-β was prepared as described in the experimental section. The Au content had a great influence on the oxidation of GLY. We studied the effect of Au content on the oxidation of GLY by preparing the Au/CuO-Sn-β with different Au content. The results were shown in Table 1. When the 1Au/2CuO-Sn-β and 1Au/3CuO-Sn-β (the number in front of Au and CuO represented the mass ratio of Au to CuO) were used as catalysts, there was a very low conversion of GLY (Table 1, Entries 1 and 2). This showed that the Au had a very low activity for the oxidation of GLY. Additionally, the selectivity to MLA was 3% and 6% for 1Au/2CuO-Sn-β and 1Au/3CuO-Sn-β respectively. This showed that both the oxidation activity of Au and the selectivity of Sn-β were affected by the Au content. Higher content of Au leads to lower conversion of GLY and lower selectivity to MLA. When

the content of CuO increased to continue to decrease the content of Au, the conversion and selectivity had a sharp increase for 1Au/4CuO-Sn-β and 1Au/5CuO-Sn-β. When the content of CuO increased to decrease the Au content further, the conversion of GLY was 67% with a 39% yield of MLA for 1Au/9CuO-Sn-β. A significant decline in both conversion and selectivity was observed on 1Au/12CuO-Sn-β. The TEM results could be used to interpret the effect of different Au content. When the content of Au was high, the large particle size of Au led to the decrease in activity for oxidation of GLY for 1Au/2CuO and 1Au/3CuO. On the contrary, the 1Au/9CuO and 1Au/12CuO with a small particle size of Au still had low oxidation activity due to the lower absolute content of Au. Therefore, an appropriate Au load was required for the high yield of MLA.

Table 1. Effect of different CuO content on GLY oxide.

Entry	Catalyst	Conversion (%)	Yield (%)	
			MLA	GLR
1	1Au/2CuO-Sn-β	6	3	1
2	1Au/3CuO-Sn-β	25	6	2
3	1Au/4CuO-Sn-β	89	56	16
4	1Au/6CuO-Sn-β	82	54	17
5	1Au/9CuO-Sn-β	67	39	12
6	1Au/12CuO-Sn-β	32	16	5

Reaction condition: glycerol (1 mmol), methanol (5 mL), catalyst (0.2000 g), O_2 (1.6 MPa), 363 K, 4 h.

2.4. Effect of Reaction Condition

2.4.1. Temperature

1Au/4CuO-Sn-β were used to study the effect of reaction temperature. The experimental results of the effect of temperature were shown in Table 2. When the reaction temperature was 343 K, the oxidation activity of the catalyst was very poor, the conversion of GLY was 53%, and the yield of MLA was 27%. The conversion of GLY gradually increased with the increase of temperature for the preparation of MLA from GLY. When the reaction temperature increased to 393 K, the conversion of GLY reached 98%. When the reaction temperature continued to increase to 413 K, the conversion of GLY remained basically unchanged. However, with the increase of reaction temperature, the yield of MLA changed significantly. When the temperature rises to 363 K, the yield of MLA increases significantly from 27% to 56%. As the reaction temperature continues to rise, the yield of MLA decreased slightly from 56% to 54%. As the reaction temperature continued to rise to 413 K, the yield of MLA decreased significantly to 32%. This should be caused by the decomposition of MLA. Considering the conversion of GLY and the yield of MLA, 363 K was determined for the following experiments.

Table 2. Effect of reaction temperature on catalytic activity.

Entry	Temperature (K)	Conversion (%)	Yield (%)	
			MLA	GLR
1	343	53	27	7
2	363	89	56	16
3	393	98	54	11
4	413	97	32	6

Reaction condition: glycerol (1 mmol), methanol (5 mL), catalyst (0.2000g), O_2 (1.6 MPa), 4 h.

2.4.2. Reaction Time

The relationship between GLY oxidation and reaction was shown in Figure 7. After reacting for 2 h, the conversion of GLY was 67%, and the yield of MLA was 34%. This indicated that the oxidation activity catalyst was higher in a short time. When the reaction time was extended to 4 h, the conversion of GLY increased from 68% to 89% while the yield of MLA increased from 34% to 56%. When the reaction time continued to increase to 6 h, the conversion of GLY was almost unchanged, and the yield of MLA increased slightly from 56% to 59%. This value was good compared to the studies on glycerol oxidation for the production of lactic acid or MLA by Au catalysts (Table 3). When the reaction time was up to 8 h, the conversion of GLY and the yield of MLA remained unchanged. This indicated that the reaction had almost reached equilibrium after 4 h. However, with the extension of reaction time, the yield of by-product GLR increased first and then decreased. The yield of GLR reached the maximum after 4 h of reaction. With the extension of reaction time, GLR should be transformed into other by-products.

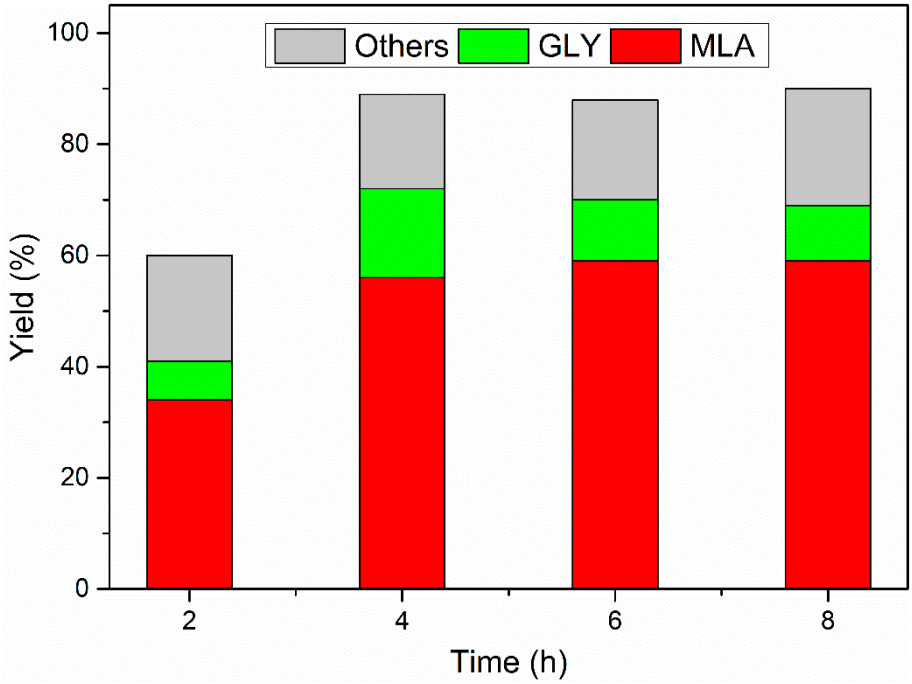

Figure 7. Effect of reaction time on catalytic activity.

Table 3. A summary of studies on glycerol oxidation to produce lactic acid or MLA by Au catalysts.

Entry	Catalyst	Product	T (K)	Conv. (%)	Sel. (%)	Yield (%)	Ref.
1	1Au/4CuO-Sn-β	MLA	363	88	67	59	This work
2	Au/USY-600	MLA	433	95	77	73	[63]
3	$AuCu/CeO_2$	lactic acid	493	78	91	71	[64]
4	$AuPt/TiO_2$	lactic acid	373	100	68	68	[65]
5	Au/CuO + Sn-MCM-41-XS	MLA	413	95	66	63	[66]
6	Au/CuO and Sn-Beta	MLA	363	86	70	60	[67]
7	Au/Sn(20)-Mt	MLA	483	78	69	54	[68]
8	Au/LPrO	lactic acid	363	68	68	46	[69]
9	Au-Pt	lactic acid	358	90	44	40	[70]
10	AuPt (15% Ptsurf)	lactic acid	r.t.	30	73	22	[40]
11	Au-Pt-ZSM-11	lactic acid	343	35	46	16	[71]

3. Materials and Methods

3.1. Materials

The CH_3OH and GLY were obtained from Tianjin FengChuan chemical reagent Technology Co., Ltd., Tianjin, China. 1,3-Dihydroxyacetone and methyl pyruvate were bought from Alfa Aesar, Haverhill, MA, USA Methyl lactate was obtained from TCI Shanghai Development Co., Ltd., Shanghai, China. NaOH and urea were obtained from Tianjin Kermel Chemical Reagent Co., Ltd., Tianjin, China. Chloroauric acid was obtained from Tianjin Fuchen Chemical Reagent Factory, Tianjin, China. Al-β was bought from Tianjin Nankai University Catalyst Factory, Tianjin, China. $SnCl_4$ was obtained from Sinopharm Chemical Reagent Co., Ltd., Shanghai, China. Tetraethyl silicate, stannous oxalate and dibutyltin maleate were bought from Shanghai Aladdin Biochemical Technology Co., Ltd. Shanghai, China. HF was obtained from Tianjin Fuyu Fine Chemical Co., Ltd., Tianjin, China.

3.2. Catalyst Synthesis

3.2.1. Preparation of Sn-β

The Sn-β molecular sieve was preparation by hydrothermal synthesis, the Sn-β with different Sn content, Sn source and water content were prepared, By changing the Sn content, Sn source and water content in the gel. Take the preparation of Sn-β with 2% content of Sn using $SnCl_4$ as the Sn source as an example. The molar composition of the gel was n(SiO_2):n(TEAOH):n (SnO_2):n (HF):n (H_2O) = 1.0:0.54:0.01:0.54:7.5. TEOS was added to tetraethyl ammonium hydroxide (TEAOH) at a uniform speed under stirring and then kept stirring for 90 min. To the mixture of tetraethyl silicate and tetraethyl ammonium hydroxide, $SnCl_4$ aqueous solution was added under stirring. After being heated and stirred at a constant temperature until the water evaporates to the required quality, a certain amount of hydrofluoric acid (HF) was added to the mixture. Then, Si-β was dispersed in water by ultra-sounded for 1 h to form a Si-β crystal seed. The gel was transferred into the quartz crucible and ground until viscous after the addition of the Si-β crystal seed. At last, the mixture was put in a crystallization kettle and kept at 413 K for 3 days. After the reaction, the solid was washed to neutral and dried at 373 k overnight. Sn-β was obtained by calcined at 823 K. The catalysts were named as Sn-β-Cl, Sn-β-OXS and Sn-β-DBTM which mean the Sn-β was prepared using $SnCl_4$, SnC_2O_4 and $C_{12}H_{20}O_4Sn$ as source respectively.

3.2.2. Preparation of Au/CuO

The Au/CuO was prepared by deposition precipitation method with nano CuO as support. Take the synthesis of 1Au/9CuO catalyst as an example; 0.8988 g copper acetate was dissolved in 180 g high-purity water, 0.78 mL of acetic acid was added and the solution was stirred for 20 min at 373 K. After the addition of 45.6 mL NaOH solution (0.3365 mol L^{-1}), the mixture was refluxed under stirring for 1 h. The mixture was cooled to room temperature, centrifuged and washed with acetone and water (20 mL + 4 mL) three times to afford the CuO. The CuO dispersed in 80 g of H_2O to be used. Then 8.4 mL of chloroauric acid solution (24.5 mmol L^{-1}) was added into a urea solution (9.76 g of urea in 120 g of H_2O) under dark. The nano CuO dispersed in high-purity water was added to the above solution and stirred at 80 °C in an oil bath in the dark for 6 h. After the reaction, the mixture was aged at room temperature for 12 h then centrifuged and washed with acetone and water (20 mL + 4 mL) three times. The sample was dried naturally, and calcined at 473 K for 5 h to obtain 1Au/9CuO. By changing the amount of copper oxide added to the support and the loading amount of Au, the prepared catalysts were expressed as 1Au/2CuO, 1Au/4CuO, 1Au/6CuO, 1Au/9CuO, 1Au/12CuO, 0.5Au/4CuO, 1.5Au/4CuO and 2Au/4CuO respectively. The number in front of Au and CuO represents the mass ratio of Au to CuO.

3.2.3. Preparation of Au/CuO-Sn-β

The calcined Au/CuO and Sn-β dispersed in acetone respectively for 3 h. Then dispersed Au/CuO was added to the dispersed Sn-β. After the acetone volatilizes completely, the sample was calcined in a muffle furnace at 473 K for 5 h. According to the Au/CuO, the prepared catalysts were labeled as 1Au/2CuO-Sn-β1Au/4CuO-Sn-β, 1Au/6CuO-Sn-β, 1Au/9CuO-Sn-β, 1Au/12CuO-Sn-β, 0.5Au/4CuO-Sn-β, 1.5Au/4CuO-Sn- β, 2Au/4CuO-Sn-β Respectively.

3.3. Characterization

The XRD patterns were collected on a PANalytical X'Pert PRO (Almelo, Netherlands) with a Cu Ka source. Tube voltage was 45 V and tube current 40 mA. The transmission electron microscopy (TEM) images were taken by a Talos F200S microscope (Waltham, MA, USA). The acceleration voltage was 200 kV. FTIR spectra of the Sn-Beta samples with pyridine adsorption were collected on a Bruker Tensor II spectrometer (Karlsruhe, Germany). Before analysis, the sample was pretreated at 723 K for 3 h in the evacuated analysis pool. After that, the spectrum as the background reference was recorded at room temperature. Then, pyridine was charged into the analysis pool to adsorb onto the sample. After about 15 min, the pool was heated to 423 K and then evacuated to desorb the pyridine. Finally, the FTIR spectrum was collected after evacuation for 30 min.

3.4. Oxidation of GLY

The reaction was conducted in stainless steel high-pressure reactor with a temperature controller to control the temperature and heating rate. The mixing speed was set at 1000 r/min by a magnetic stirrer. In a typical procedure, GLY (1 mmol), CH_3OH (5 mL) and magneton were put into the reactor. After replacing the air with oxygen six times, the reactor was filled with 1.6 MPa of O_2. The specified temperature was reached, the reaction was started by turning on the agitator. After the reaction, the reactor was cooled to room temperature. The reaction solution was centrifuged and the reactor and catalyst were washed with a small amount of methanol many times. The products were analyzed by adding internal standards (naphthalene).

4. Conclusions

In conclusion, the conversion of glycerol to methyl lactate was realized by the combined action of Au/CuO and Sn-β. The addition of Sn, which leads to the introduction of L-acid sites in the zeolite, played a key role in the high selectivity to methyl lactate. $SnCl_4$ was proved to be the promising Sn source candidate for this conversion. The size of Au particles increased with the increase of the content of Au. The method of mixing Au/CuO and Sn-β for the preparation of Au/CuO-Sn-β did not damage the structure of Sn-β. After optimization of reaction conditions, a 59% yield of methyl lactate from glycerol was achieved.

Supplementary Materials: The following are available online at https://www.mdpi.com/article/10.3390/catal12010104/s1, Figure S1: TEM image of 1Au/4CuO-Sn-β, Figure S2: The XRD patterns of Sn-β-Cl prepared the content of H_2O at H_2O/SiO_2 = 7.5, Table S1: Effects of $SnCl_4$ as Tin Source on the Catalytic Performance, Table S2: Effect of SnC_2O_4 as Sn source and Sn content on catalytic performance, Table S3: Effect of $C_{12}H_{20}O_4Sn$ as tin source and Sn content on catalytic performance, Table S4: Effect of amplified synthesis of Sn-β on the catalytic performance.

Author Contributions: Conceptualization, T.L. and C.X.; methodology, Y.D.; validation, Q.L. and R.N.; investigation, Y.D.; data curation, J.W.; writing—original draft preparation, Y.D.; writing—review and editing, T.L.; visualization, Y.Z.; supervision, C.X.; project administration, T.L. and C.X.; funding acquisition, T.L. and Y.D. All authors have read and agreed to the published version of the manuscript.

Funding: This research was funded by the National Natural Science Foundation of China (21802125 and 21801110).

Conflicts of Interest: The authors declare no conflict of interest.

References

1. Xu, C.; Paone, E.; Rodriguez-Padron, D.; Luque, R.; Mauriello, F. Recent catalytic routes for the preparation and the upgrading of biomass derived furfural and 5-hydroxymethylfurfural. *Chem. Soc. Rev.* **2020**, *49*, 4273–4306. [CrossRef] [PubMed]
2. Besson, M.; Gallezot, P.; Pinel, C. Conversion of biomass into chemicals over metal catalysts. *Chem. Rev.* **2014**, *114*, 1827–1870. [CrossRef] [PubMed]
3. Corma, A.; Iborra, S.; Velty, A. Chemical routes for the transformation of biomass into chemicals. *Chem. Rev.* **2007**, *107*, 2411–2502. [CrossRef] [PubMed]
4. Mika, L.T.; Cséfalvay, E.; Németh, Á. Catalytic conversion of carbohydrates to initial platform chemicals: Chemistry and sustainability. *Chem. Rev.* **2017**, *118*, 506–613. [CrossRef]
5. Duan, Y.; Zhang, J.; Li, D.; Deng, D.; Ma, L.-F.; Yang, Y. Direct conversion of carbohydrates to diol by the combination of niobic acid and a hydrophobic ruthenium catalyst. *RSC Adv.* **2017**, *7*, 26487–26493. [CrossRef]
6. Fulignati, S.; Antonetti, C.; Wilbers, E.; Licursi, D.; Heeres, H.J.; Raspolli Galletti, A.M. Tunable HMF hydrogenation to furan diols in a flow reactor using Ru/C as catalyst. *J. Ind. Eng. Chem.* **2021**, *100*, 390.e1. [CrossRef]
7. Lei, N.; Zhao, X.; Hou, B.; Yang, M.; Zhou, M.; Liu, F.; Wang, A.; Zhang, T. Effective hydrogenolysis of glycerol to 1,3-propanediol over metal-acid concerted Pt/WOx /Al_2O_3 Catalysts. *ChemCatChem* **2019**, *11*, 3903–3912. [CrossRef]
8. Date, N.S.; Chikate, R.C.; Roh, H.-S.; Rode, C.V. Bifunctional role of Pd/MMT-K 10 catalyst in direct transformation of furfural to 1,2-pentanediol. *Catal. Today* **2018**, *309*, 195–201. [CrossRef]
9. Amaniampong, P.N.; Trinh, Q.T.; Varghese, J.J.; Behling, R.; Valange, S.; Mushrif, S.H.; Jerome, F. Unraveling the mechanism of the oxidation of glycerol to dicarboxylic acids over a sonochemically synthesized copper oxide catalyst. *Green Chem.* **2018**, *20*, 2730–2741. [CrossRef]
10. Han, X.; Li, C.; Guo, Y.; Liu, X.; Zhang, Y.; Wang, Y. N-doped carbon supported Pt catalyst for base-free oxidation of 5-hydroxymethylfurfural to 2,5-furandicarboxylic acid. *Appl. Catal. A: Gen.* **2016**, *526*, 1–8. [CrossRef]
11. Davidson, M.G.; Elgie, S.; Parsons, S.; Young, T.J. Production of HMF, FDCA and their derived products: A review of life cycle assessment (LCA) and techno-economic analysis (TEA) studies. *Green Chem.* **2021**, *23*, 3154–3171. [CrossRef]
12. Sajid, M.; Zhao, X.B.; Liu, D.H. Production of 2,5-furandicarboxylic acid (FDCA) from 5-hydroxymethylfurfural (HMF): Recent progress focusing on the chemical-catalytic routes. *Green Chem.* **2018**, *20*, 5427–5453. [CrossRef]
13. Zhang, J.; Jia, W.L.; Sun, Y.; Yang, S.L.; Tang, X.; Zeng, X.H.; Lin, L. An efficient approach to synthesizing 2,5-bis(N-methyl-aminomethyl)furan from 5-hydroxymethylfurfural via 2,5-bis(N-methyl-iminomethyl)furan using a two-step reaction in one pot. *Green Chem.* **2021**, *23*, 5656–5664. [CrossRef]
14. Sha, J.; Kusema, B.T.; Zhou, W.J.; Yan, Z.; Streiff, S.; Pera-Titus, M. Single-reactor tandem oxidation-amination process for the synthesis of furan diamines from 5-hydroxymethylfurfural. *Green Chem.* **2021**, *23*, 7093–7099. [CrossRef]
15. Xu, Y.M.; Jia, X.Q.; Ma, J.P.; Gao, J.; Xia, F.; Li, X.F.; Xu, J. Selective synthesis of 2,5-bis(aminomethyl) furan via enhancing the catalytic dehydrationhydrogenation of 2,5-diformylfuran dioxime. *Green Chem.* **2018**, *20*, 2697–2701. [CrossRef]
16. Yang, Y.; Xie, Y.; Deng, D.; Li, D.; Zheng, M.; Duan, Y. Highly selective conversion of HMF to 1-hydroxy- 2,5-hexanedione on Pd/MIL-101(Cr). *ChemistrySelect* **2019**, *4*, 11165–11171. [CrossRef]
17. Duan, Y.; Zheng, M.; Li, D.; Deng, D.; Ma, L.-F.; Yang, Y. Conversion of HMF to methyl cyclopentenolone by the Pd/Nb_2O_5 and Ca-Al catalysts via two-steps procedure. *Green Chem.* **2017**, *19*, 5103–5113. [CrossRef]
18. Zhou, X.; Feng, Z.; Guo, W.; Liu, J.; Li, R.; Chen, R.; Huang, J. Hydrogenation and hydrolysis of furfural to furfuryl alcohol, cyclopentanone, and cyclopentanol with a heterogeneous copper catalyst in water. *Ind. Eng. Chem. Res.* **2019**, *58*, 3988–3993. [CrossRef]
19. Li, Y.; Guo, X.; Liu, D.; Mu, X.; Chen, X.; Shi, Y. Selective conversion of furfural to cyclopentanone or cyclopentanol using Co-Ni catalyst in water. *Catalysts* **2018**, *8*, 193. [CrossRef]
20. Yang, Y.; Yang, D.; Zhang, C.; Zheng, M.; Duan, Y. Preparation of 1-hydroxy-2,5-hexanedione from HMF by the combination of commercial Pd/C and acetic acid. *Molecules* **2020**, *25*, 2475. [CrossRef]
21. Thananatthanachon, T.; Rauchfuss, T.B. Efficient production of the liquid fuel 2,5-dimethylfuran from fructose using formic acid as a reagent. *Angew. Chem. Int. Edit.* **2010**, *49*, 6616–6618. [CrossRef]
22. Roman-Leshkov, Y.; Barrett, C.J.; Liu, Z.Y.; Dumesic, J.A. Production of dimethylfuran for liquid fuels from biomass-derived carbohydrates. *Nature* **2007**, *447*, 982–985. [CrossRef]
23. Zhang, S.D.; Liu, Y.X.; Yang, S.; Li, H. Catalytic upgrading of bio-based 5-hydroxymethylfurfural to 2,5-dimethylfuran with non-noble metals. *Energy Technol.* **2021**, *9*, 2100653. [CrossRef]
24. Atabani, A.E.; Silitonga, A.S.; Badruddin, I.A.; Mahlia, T.M.I.; Masjuki, H.H.; Mekhilef, S. A comprehensive review on biodiesel as an alternative energy resource and its characteristics. *Renew. Sustain. Energy Rev.* **2012**, *16*, 2070–2093. [CrossRef]
25. Hoekman, S.K.; Broch, A.; Robbins, C.; Ceniceros, E.; Natarajan, M. Review of biodiesel composition, properties, and specifications. *Renew. Sustain. Energy Rev.* **2012**, *16*, 143–169. [CrossRef]
26. Miao, G.; Shi, L.; Zhou, Z.M.; Zhu, L.J.; Zhang, Y.F.; Zhao, X.P.; Luo, H.; Li, S.G.; Kong, L.Z.; Sun, Y.H. Catalyst design for selective hydrodeoxygenation of glycerol to 1,3-propanediol. *ACS Catal.* **2020**, *10*, 15217–15226. [CrossRef]

27. Sun, S.Q.; Shu, L.; Lu, X.Y.; Wang, Q.H.; Tisma, M.; Zhu, C.G.; Shi, J.P.; Baganz, F.; Lye, G.J.; Hao, J. 1,2-Propanediol production from glycerol via an endogenous pathway of Klebsiella pneumoniae. *Appl. Microbiol. Biotechnol.* **2021**, *105*, 9003–9016. [CrossRef]
28. Gabrysch, T.; Peng, B.X.; Bunea, S.; Dyker, G.; Muhler, M. The role of metallic copper in the selective hydrodeoxygenation of glycerol to 1,2-propanediol over Cu/ZrO_2. *ChemCatChem* **2018**, *10*, 1344–1350. [CrossRef]
29. Bharath, G.; Rambabu, K.; Hai, A.; Taher, H.; Banat, F. Development of Au and 1D hydroxyapatite nanohybrids supported on 2D boron nitride sheets as highly efficient catalysts for dehydrogenating glycerol to lactic acid. *ACS Sustain. Chem. Eng.* **2020**, *8*, 7278–7289. [CrossRef]
30. Razali, N.; Abdullah, A.Z. Production of lactic acid from glycerol via chemical conversion using solid catalyst: A review. *Appl. Catal. A Gen.* **2017**, *543*, 234–246. [CrossRef]
31. Torres, S.; Palacio, R.; Lopez, D. Support effect in Co_3O_4-based catalysts for selective partial oxidation of glycerol to lactic acid. *Appl. Catal. A Gen.* **2021**, *621*, 118199. [CrossRef]
32. Qiu, K.B.; Shu, Y.X.; Zhang, J.; Gao, L.J.; Xiao, G.M. Effective and stable zeolite imidazole framework-supported copper nanoparticles (Cu/ZIF-8) for glycerol to lactic acid. *Catal. Lett.* **2021**, *152*, 172–186. [CrossRef]
33. Palacio, R.; Torres, S.; Lopez, D.; Hernandez, D. Selective glycerol conversion to lactic acid on Co_3O_4/CeO_2 catalysts. *Catal. Today* **2018**, *302*, 196–202. [CrossRef]
34. Zavrazhnov, S.A.; Esipovich, A.L.; Zlobin, S.Y.; Belousov, A.S.; Vorotyntsev, A.V. Mechanism analysis and kinetic modelling of Cu NPs catalysed glycerol conversion into lactic acid. *Catalysts* **2019**, *9*, 231. [CrossRef]
35. Siddiki, S.; Touchy, A.S.; Kon, K.; Toyao, T.; Shimizu, K. Oxidant-free dehydrogenation of glycerol to lactic acid by heterogeneous platinum catalysts. *ChemCatChem* **2017**, *9*, 2816–2821. [CrossRef]
36. Shen, Y.H.; Zhang, S.H.; Li, H.J.; Ren, Y.; Liu, H.C. Efficient synthesis of lactic acid by aerobic oxidation of glycerol on $Au-Pt/TiO_2$ catalysts. *Chem. A Eur. J.* **2010**, *16*, 7368–7371. [CrossRef]
37. Zhang, C.; Wang, T.; Liu, X.; Ding, Y.J. Selective oxidation of glycerol to lactic acid over activated carbon supported Pt catalyst in alkaline solution. *Chin. J. Catal.* **2016**, *37*, 502–509. [CrossRef]
38. Palacio, R.; Torres, S.; Royer, S.; Mamede, A.S.; Lopez, D.; Hernandez, D. CuO/CeO_2 catalysts for glycerol selective conversion to lactic acid. *Dalton Trans.* **2018**, *47*, 4572–4582. [CrossRef]
39. Zhang, G.Y.; Jin, X.; Guan, Y.N.; Yin, B.; Chen, X.B.; Liu, Y.B.; Feng, X.; Shan, H.H.; Yang, C.H. Toward selective dehydrogenation of glycerol to lactic acid over bimetallic Pt-Co/CeOx catalysts. *Ind. Eng. Chem. Res.* **2019**, *58*, 14548–14558. [CrossRef]
40. Dai, C.C.; Sun, L.B.; Liao, H.B.; Khezri, B.; Webster, R.D.; Fisher, A.C.; Xu, Z.C.J. Electrochemical production of lactic acid from glycerol oxidation catalyzed by AuPt nanoparticles. *J. Catal.* **2017**, *356*, 14–21. [CrossRef]
41. Abdullah, A.Z.; Yaacob, M.H.; Basir, N.I. Synergy between oxides of Ni and Ca for selective catalytic lactic acid synthesis from glycerol in a single step process. *J. Ind. Eng. Chem.* **2020**, *85*, 282–288. [CrossRef]
42. Yin, H.X.; Yin, H.B.; Wang, A.L.; Shen, L.Q. Catalytic conversion of glycerol to lactic acid over graphite-supported nickel nanoparticles and reaction kinetics. *J. Ind. Eng. Chem.* **2018**, *57*, 226–235. [CrossRef]
43. Sharninghausen, L.S.; Campos, J.; Manas, M.G.; Crabtree, R.H. Efficient selective and atom economic catalytic conversion of glycerol to lactic acid. *Nat. Commun.* **2014**, *5*, 5084. [CrossRef] [PubMed]
44. Lu, T.L.; Fu, X.M.; Zhou, L.P.; Su, Y.L.; Yang, X.M.; Han, L.; Wang, J.F.; Song, C.Y. Promotion effect of Sn on Au/Sn-USY catalysts for one-pot conversion of glycerol to methyl lactate. *ACS Catal.* **2017**, *7*, 7274–7284. [CrossRef]
45. Kwon, Y.; Birdja, Y.; Spanos, I.; Rodriguez, P.; Koper, M.T.M. Highly selective electro-oxidation of glycerol to dihydroxyacetone on platinum in the presence of bismuth. *ACS Catal.* **2012**, *2*, 759–764. [CrossRef]
46. Xiao, Y.; Greeley, J.; Varma, A.; Zhao, Z.J.; Xiao, G.M. An experimental and theoretical study of glycerol oxidation to 1,3-dihydroxyacetone over bimetallic Pt-Bi catalysts. *AlChE J.* **2017**, *63*, 705–715. [CrossRef]
47. Zhang, Y.H.; Zhang, N.; Tang, Z.R.; Xu, Y.J. Identification of Bi2WO6 as a highly selective visible-light photocatalyst toward oxidation of glycerol to dihydroxyacetone in water. *Chem. Sci.* **2013**, *4*, 1820–1824. [CrossRef]
48. An, Z.; Ma, H.H.; Han, H.B.; Huang, Z.Y.; Jiang, Y.T.; Wang, W.L.; Zhu, Y.R.; Song, H.Y.; Shu, X.; Xiang, X.; et al. Insights into the multiple synergies of supports in the selective oxidation of glycerol to dihydroxyacetone: Layered double hydroxide supported Au. *ACS Catal.* **2020**, *10*, 12437–12453. [CrossRef]
49. Duan, X.Z.; Zhang, Y.F.; Pan, M.J.; Dong, H.; Chen, B.X.; Ma, Y.Y.; Qian, G.; Zhou, X.G.; Yang, J.; Chen, D. SbOx-promoted Pt nanoparticles supported on CNTs as catalysts for base-free oxidation of glycerol to dihydroxyacetone. *AlChE J.* **2018**, *64*, 3979–3987. [CrossRef]
50. Walgode, P.M.; Faria, R.P.V.; Rodrigues, A.E. A review of aerobic glycerol oxidation processes using heterogeneous catalysts: A sustainable pathway for the production of dihydroxyacetone. *Catal. Rev.* **2021**, *63*, 422–511. [CrossRef]
51. Hirasawa, S.; Nakagawa, Y.; Tomishige, K. Selective oxidation of glycerol to dihydroxyacetone over a Pd-Ag catalyst. *Catal. Sci. Technol.* **2012**, *2*, 1150–1152. [CrossRef]
52. Hirasawa, S.; Watanabe, H.; Kizuka, T.; Nakagawa, Y.; Tomishige, K. Performance, structure and mechanism of Pd-Ag alloy catalyst for selective oxidation of glycerol to dihydroxyacetone. *J. Catal.* **2013**, *300*, 205–216. [CrossRef]
53. Tan, H.; Yao, C.J.; Zhan, T.; Li, W.Q.; Zhu, J.P.; Wang, G.; Liu, W.B.; Sun, M.T.; Wang, S.H. Selective oxidation of glycerol to dihydroxyacetone over N-doped porous carbon stabilized CuxO supported Au catalysts. *Mol. Catal.* **2020**, *498*, 111243. [CrossRef]
54. Ning, X.M.; Zhan, L.; Wang, H.J.; Yu, H.; Peng, F. Deactivation and regeneration of in situ formed bismuth-promoted platinum catalyst for the selective oxidation of glycerol to dihydroxyacetone. *New J. Chem.* **2018**, *42*, 18837–18843. [CrossRef]

55. Carrettin, S.; McMorn, P.; Johnston, P.; Griffin, K.; Hutchings, G.J. Selective oxidation of glycerol to glyceric acid using a gold catalyst in aqueous sodium hydroxide. *Chem. Commun.* **2002**, 696–697. [CrossRef]
56. Ke, Y.H.; Li, X.H.; Li, J.F.; Liu, C.L.; Xu, C.L.; Dong, W.S. Conversion of glycerol to dihydroxyacetone over Au catalysts on various supports. *J. Chem. Technol. Biotechnol.* **2020**, *95*, 1153–1162. [CrossRef]
57. Innocenti, G.; Papadopoulos, E.; Fornasari, G.; Cavani, F.; Medford, A.J.; Sievers, C. Continuous liquid-phase upgrading of dihydroxyacetone to lactic acid over metal phosphate catalysts. *ACS Catal.* **2020**, *10*, 11936–11950. [CrossRef]
58. Hossain, M.A.; Mills, K.N.; Molley, A.M.; Rahaman, M.S.; Tulaphol, S.; Lalvani, S.B.; Dong, J.; Sunkara, M.K.; Sathitsuksanoh, N. Catalytic isomerization of dihydroxyacetone to lactic acid by heat treated zeolites. *Appl. Catal. A Gen.* **2021**, *611*, 117979. [CrossRef]
59. Jolimaitre, E.; Delcroix, D.; Essayem, N.; Pinel, C.; Besson, M. Dihydroxyacetone conversion into lactic acid in an aqueous medium in the presence of metal salts: Influence of the ionic thermodynamic equilibrium on the reaction performance. *Catal. Sci. Technol.* **2018**, *8*, 1349–1356. [CrossRef]
60. Sobus, N.; Czekaj, I. Comparison of synthetic and natural zeolite catalysts' behavior in the production of lactic acid and ethyl lactate from biomass-derived dihydroxyacetone. *Catalysts* **2021**, *11*, 1006. [CrossRef]
61. Wang, X.C.; Liang, F.B.; Huang, C.P.; Li, Y.X.; Chen, B.H. Siliceous tin phosphates as effective bifunctional catalysts for selective conversion of dihydroxyacetone to lactic acid. *Catal. Sci. Technol.* **2016**, *6*, 6551–6560. [CrossRef]
62. Feliczak-Guzik, A.; Sprynskyy, M.; Nowak, I.; Buszewski, B. Catalytic isomerization of dihydroxyacetone to lactic acid and alkyl lactates over hierarchical zeolites containing tin. *Catalysts* **2018**, *8*, 31. [CrossRef]
63. Pazhavelikkakath Purushothaman, R.K.; van Haveren, J.; Melian-Cabrera, I.; van Eck, E.R.; Heeres, H.J. Base-free, one-pot chemocatalytic conversion of glycerol to methyl lactate using supported gold catalysts. *ChemSusChem* **2014**, *7*, 1140–1147. [CrossRef]
64. Palacio, R.; López, D.; Hernández, D. Bimetallic AuCu nanoparticles supported on CeO2 as selective catalysts for glycerol conversion to lactic acid in aqueous basic medium. *J. Nanopart. Res.* **2019**, *21*, 148. [CrossRef]
65. Evans, C.D.; Douthwaite, M.; Carter, J.H.; Pattisson, S.; Kondrat, S.A.; Bethell, D.; Knight, D.W.; Taylor, S.H.; Hutchings, G.J. Enhancing the understanding of the glycerol to lactic acid reaction mechanism over AuPt/ TiO_2 under alkaline conditions. *J. Chem. Phys.* **2020**, *152*, 134705. [CrossRef] [PubMed]
66. Tang, Z.; Fiorilli, S.L.; Heeres, H.J.; Pescarmona, P.P. Multifunctional heterogeneous catalysts for the selective conversion of glycerol into methyl lactate. *ACS Sustain. Chem. Eng.* **2018**, *6*, 10923–10933. [CrossRef]
67. Zhou, L.; Xu, Y.; Yang, X.; Lu, T.; Han, L. Utilization of biodiesel byproduct glycerol: Production of methyl lactate over Au/CuO and Sn-Beta binary catalyst under mild reaction conditions. *Energy Convers. Manag.* **2019**, *196*, 277–285. [CrossRef]
68. Li, J.; Li, D.; Liu, C.L.; Xu, C.; Dong, W.S. The conversion of glycerol to methyl lactate catalyzed by tin-exchanged montmorillonite-supported gold catalysts. *J. Chem. Technol. Biot.* **2019**, *94*, 1958–1967. [CrossRef]
69. Wang, C.; Zhang, X.; Li, J.; Qi, X.; Guo, Z.; Wei, H.; Chu, H. Gold nanoparticles on nanosheets derived from layered rare-earth hydroxides for catalytic glycerol-to-lactic acid conversion. *ACS Appl. Mater. Interfaces.* **2021**, *13*, 522–530. [CrossRef]
70. Mimura, N.; Muramatsu, N.; Hiyoshi, N.; Sato, O.; Yamaguchi, A. Continuous production of glyceric acid and lactic acid by catalytic oxidation of glycerol over an Au-Pt/Al_2O_3 bimetallic catalyst using a liquid-phase flow reactor. *Catal. Today* **2021**, *375*, 191–196. [CrossRef]
71. Diguilio, E.; Renzini, M.S.; Pierella, L.B.; Domine, M.E. Conversion of glycerol to value added products in a semi-continuous batch reactor using noble metals supported on ZSM-11 zeolite. *Nanomaterials* **2021**, *11*, 510. [CrossRef] [PubMed]